



Climate Sensitivity of the Community Climate System Model, Version 4

C. M. BITZ

Atmospheric Sciences, University of Washington, Seattle, Washington

K. M. SHELL

College of Oceanic and Atmospheric Sciences, Oregon State University, Corvallis, Oregon

P. R. GENT, D. A. BAILEY, AND G. DANABASOGLU

National Center for Atmospheric Research, Boulder, Colorado

K. C. ARMOUR

Atmospheric Sciences, University of Washington, Seattle, Washington

M. M. HOLLAND AND J. T. KIEHL

National Center for Atmospheric Research, Boulder, Colorado

(Manuscript received 23 May 2011, in final form 3 November 2011)

ABSTRACT

Equilibrium climate sensitivity of the Community Climate System Model, version 4 (CCSM4) is 3.20°C for 1° horizontal resolution in each component. This is about a half degree Celsius higher than in the previous version (CCSM3). The transient climate sensitivity of CCSM4 at 1° resolution is 1.72°C, which is about 0.2°C higher than in CCSM3. These higher climate sensitivities in CCSM4 cannot be explained by the change to a preindustrial baseline climate. This study uses the radiative kernel technique to show that, from CCSM3 to CCSM4, the global mean lapse-rate feedback declines in magnitude and the shortwave cloud feedback increases. These two warming effects are partially canceled by cooling because of slight decreases in the global mean water vapor feedback and longwave cloud feedback from CCSM3 to CCSM4.

A new formulation of the mixed layer, slab-ocean model in CCSM4 attempts to reproduce the SST and sea ice climatology from an integration with a full-depth ocean, and it is integrated with a dynamic sea ice model. These new features allow an isolation of the influence of ocean dynamical changes on the climate response when comparing integrations with the slab ocean and full-depth ocean. The transient climate response of the full-depth ocean version is 0.54 of the equilibrium climate sensitivity when estimated with the new slab-ocean model version for both CCSM3 and CCSM4. The authors argue the ratio is the same in both versions because they have about the same zonal mean pattern of change in ocean surface heat flux, which broadly resembles the zonal mean pattern of net feedback strength.

1. Introduction

Equilibrium climate sensitivity (ECS) is an often used metric to evaluate the climate response to a perturbation in the radiative forcing. It is specifically defined as the equilibrium change in global mean surface air

temperature that results from doubling the concentration of carbon dioxide (CO₂) in the atmosphere (IPCC 1990). In this study we investigate how the new Community Climate System Model, version 4 (CCSM4) responds to doubling CO₂ compared to the previous version (CCSM3) by evaluating ECS and the regional climate response when the models are integrated with a slab-ocean model. We also examine the transient response in multcentury integrations of idealized CO₂-doubling experiments of CCSM3 and CCSM4 with a full-depth, ocean general circulation model (OGCM).

Corresponding author address: C. M. Bitz, Atmospheric Sciences, University of Washington, NE Campus Parkway, Seattle, WA 98195-5852.

E-mail: bitz@atmos.washington.edu

The CCSM3 was used extensively for climate studies documented in the Intergovernmental Panel on Climate Change (IPCC) Fourth Assessment Report (AR4) (e.g., Randall et al. 2007) and, in subsequent years, by the wider community. By comparing climate sensitivity in CCSM3 and CCSM4 for standard idealized CO₂ doubling experiments, we gain a deeper understanding of the new model by referencing it to other models we know well. We also aim to learn how the new model will compare to the larger body of climate models that will be part of IPCC AR5.

An estimate of the ECS in climate models with an OGCM requires very long simulations (thousands of years) to achieve a steady state. Climate models are rarely run long enough, and instead the ECS is usually approximated from a climate model with a mixed layer ocean model, which we call a slab-ocean model (SOM), with prescribed, annually periodic ocean heat transport.

Typically the SOM is designed to reproduce observed SST and sea ice cover (e.g., McFarlane et al. 1992; Kiehl et al. 2006; Knutson 2009; Schmidt et al. 2006). However, reproducing observations rather than the mean state of the climate model with an OGCM has two undesirable side effects for estimating ECS as well as the regional climate response to doubling CO₂. The first is that the mean climate may differ substantially for the same climate model with SOM versus OGCM. Boer and Yu (2003a) and Boer and Yu (2003c) show that the mean climate influences the pattern of temperature response and effective climate sensitivity (an estimate of ECS from transient integrations, see section 4), and hence the equilibrium response to doubling CO₂ may differ for the same climate model with a SOM versus OGCM. The second is that it is difficult to simulate accurately the sea ice covered seas because observations of the sea ice mass balance are inadequate to construct needed input to the SOM. CCSM3's standard SOM has motionless sea ice to simplify the problem. Even so, the sea ice thickness pattern can be unlike nature, and yet the base-state thickness is known to significantly affect sea ice response in climate models (Holland and Bitz 2003; Bitz and Roe 2004; Bitz 2008).

The slab-ocean model in the CCSM4 has been revised substantially to remedy both of these problems, and now it reproduces well the SST and sea ice of the CCSM4 with the full OGCM and uses the full physics of the sea ice component model. (In fact, the same sea ice physics must be used with the SOM as in the OGCM.) The new SOM permits a fruitful comparison of the climate model run with SOM and OGCM as a way to evaluate the role of ocean dynamics, as has already been done by Bitz et al. (2006) and McCusker et al. (2012) with the new SOM implemented in CCSM3. Several other climate

TABLE 1. Model configurations used in this study.

Configuration	Description
CCSM3-OLDSOM	Complete atmosphere and land components, thermodynamic-only sea ice and slab ocean as in Kiehl et al. (2006)
CCSM3-NEWSOM	Complete atmosphere, land, and sea ice components, and slab ocean as in section 2b
CCSM4-NEWSOM	Complete atmosphere, land, and sea ice components, and slab ocean as in section 2b
CCSM3-OGCM	Complete atmosphere, land, sea ice, and ocean components
CCSM4-OGCM	Complete atmosphere, land, sea ice, and ocean components

models have had full sea ice physics in their SOMs before CCSM4 (e.g., Knutson 2009; Schmidt et al. 2006).

In this study we evaluate the dependence of ECS on several new features in the CCSM4 atmosphere and land component models as well as the SOM formulation. The ECS in CCSM4 is defined relative to 1850-level CO₂, rather than the present-day level as was done in CCSM3. We explore the consequences of this change in baseline CO₂ as well. Spatial patterns of a variety of climate variables along with radiative kernel feedback analysis are used to investigate model differences. For both CCSM3 and CCSM4, we compare the transient climate response in the models with an OGCM to the ECS.

2. Model descriptions

The CCSM3 and CCSM4 are well described by Collins et al. (2006) and Gent et al. (2011), respectively, so we only briefly summarize the new aspects of CCSM4 that might affect climate sensitivity in section 2a. Because we find the SOM formulation has a considerable effect on ECS, we go into greater depth about the SOM in section 2b. Experimental details and a brief description of the surface climate in the SOM models are given in sections 2c and 2d, respectively.

Table 1 summarizes the configurations of the model that are used in this study.

a. Model changes relevant to climate sensitivity

The CCSM4 is made up of the Community Atmosphere Model version 4 (CAM4), the Community Land Model version 4 (CLM4), the sea ice component version 4 (CICE4), and the Parallel Ocean Program version 2 (POP2).

The atmosphere model has a newly revised version of the Zhang and McFarlane (1995) deep convection scheme that allows an ascending convective parcel to

mix with its environment, a so-called dilute-mixing assumption (Neale et al. 2008). CAM4 now includes the effects of deep convection in the momentum equation, which has been shown to reduce many of the biases in the surface winds, tropical convection, and the Hadley circulation in CAM3 (Richter and Rasch 2008). The low cloud fraction in cold, dry conditions has been reduced by the inclusion of a new parameterization called “freeze-dry” (Vavrus and Waliser 2008). These and other changes to CAM4 are documented in Neale et al. (2010).

The changes in CLM4 that are most relevant to climate sensitivity are the addition of a carbon–nitrogen (CN) cycling and modifications to assumptions about how snow covers vegetation. These and other changes to CLM4 are documented in Lawrence et al. (2012). The CN cycling involves a prognostic calculation of carbon and nitrogen in vegetative and soil processes, with time-varying leaf area and vegetation height. The CN cycling is a slow process compared to most processes that have traditionally been included in estimates of ECS (e.g., see Lunt et al. 2010). Both CN cycling and the new snow burial parameterizations affect surface albedo and are therefore candidates to affect climate sensitivity. However, we tested the sensitivity to CN cycling in isolation and found it had a negligible effect on ECS. We do not present these results below because the tests used a predecessor to the Q_{fix} used in all the other CCSM4 integrations described in this paper.

The primary change to CICE4 is the new multiple-scattering radiative transfer scheme of Briegleb and Light (2007). This scheme requires a melt pond fractional coverage, which has been parameterized as outlined in Holland et al. (2012).

There are numerous changes to POP2 that affect results we discuss in section 4 and, in so far as they alter the mean state SST, integrations with the SOM. The vertical resolution of the ocean increased from 40 to 60 levels from CCSM3 to CCSM4, which improves the thermocline structure and the SST. In CCSM4, the Labrador Sea convection site is in better agreement with observations than in CCSM3, most likely owing to the new overflow parameterization and reduced horizontal viscosities in CCSM4. Adjustments to mesoscale and vertical mixing and the addition of a new submesoscale mixing scheme all influence mixed layer depths, surface heat fluxes, and ocean temperature change in response to climate perturbations. These and other changes to POP2 in CCSM4 are described by Danabasoglu et al. (2012).

b. Changes to the slab-ocean model

A slab-ocean model treats the ocean as motionless but perfectly mixed throughout its depth. The primary challenge is to construct an ocean heat transport convergence

that can be prescribed in the SOM to achieve a desirable mean climate. We refer to this heat transport convergence as a Q_{fix} . To estimate ECS, the Q_{fix} should be annually periodic, and the Q_{fix} should not differ between integrations with different radiative forcings.

Estimating the Q_{fix} typically involves a special integration procedure. At least two methods have been employed in the past. One is to perform an Atmospheric Model Intercomparison (AMIP)-type experiment where the atmosphere and land components are integrated with prescribed climatologies of SST and sea ice concentration and thickness. The Q_{fix} is derived from the net surface fluxes, with corrections in sea ice-covered seas based on estimates of the sea ice mass budget. This technique is used in the SOM in the standard CCSM3, which we refer to as the OLDSOM, and in models from the Canadian Centre for Climate Modeling and Analysis (McFarlane et al. 1992) and National Aeronautics and Space Administration (NASA)/Goddard Institute for Space Studies (Schmidt et al. 2006). A second method is to run an integration with the SOM initially with zero Q_{fix} but with SST and sea ice concentration and thickness restored to climatology. The climatology of the restoring flux is then the Q_{fix} in subsequent SOM runs. This method is used by the Geophysical Fluid Dynamics Laboratory (Knutson 2009) and the Hadley Centre (Williams et al. 2000) models.

The new slab-ocean model, which we refer to as the NEWSOM, is the standard in CCSM4. The CCSM4-NEWSOM is intended to reproduce the SST and sea ice of the CCSM4-OGCM, so the Q_{fix} is constructed from a 20-yr climatology of SST, mixed-layer depth, and fluxes from a long control of the CCSM4-OGCM at the same resolution as the CCSM4-NEWSOM, using

$$\rho_o c_p h \frac{\partial \text{SST}}{\partial t} = F_{\text{net}} + Q_{\text{fix}}, \quad (1)$$

where ρ_o is the density of seawater, c_p is the ocean heat capacity, and h is the mixed layer depth. The net heat flux into the ocean F_{net} includes the atmosphere-to-ocean and ocean-to-sea ice basal and lateral surface fluxes and sensible (if any) and latent heat from snow falling into the ocean and sea ice growing over open ocean, and “runoff” (which includes land ice calving). The Q_{fix} constructed this way is so accurate that no adjustments are needed in CCSM4-NEWSOM.

The CCSM4-NEWSOM must employ the same sea ice physics of the long control run from which F_{net} is derived, which is normally the full, dynamic–thermodynamic sea ice component model of CCSM4-OGCM, with ocean drag on the sea ice computed from prescribed ocean surface currents from a CCSM4 climatology. The CCSM4-NEWSOM is intended to more closely approximate the

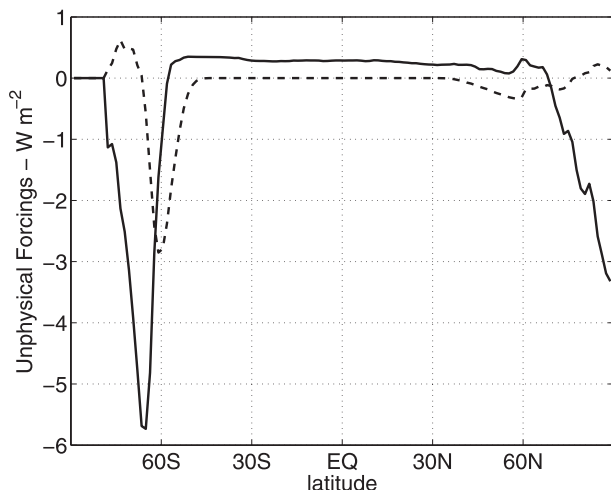


FIG. 1. Zonal mean climate forcing resulting from on-the-fly adjustments to the Q_{fix} (solid) and from neglecting the latent heat of snow falling into the ocean (dashed) from doubling CO_2 CCSM3-OLDSOM at T85.

ECS of the CCSM4-OGCM. The NEWSOM was originally implemented in CCSM3 with results shown in Holland et al. (2006), Bitz et al. (2006), and Bitz (2008), but it was not in an official release of the CCSM3. In the CCSM3-NEWSOM, the Q_{fix} is computed from a 20-yr climatology taken from a long control of the CCSM3-OGCM at the same resolution as the CCSM3-NEWSOM.

In contrast, in the CCSM3-OLDSOM, F_{net} is not well constrained in the presence of sea ice because the ocean-to-sea ice fluxes are not known to sufficient accuracy from observations to yield a reasonable sea ice mass balance. A first attempt at estimating the Q_{fix} gave poor results in sea ice-covered seas; therefore, additional adjustments to the Q_{fix} are made in the presence of sea ice. In the CCSM3-OLDSOM these are continuously computed in the slab ocean and typically amount to about $5\text{--}10 \text{ W m}^{-2}$ in the ice covered seas. A further global adjustment is made to the Q_{fix} to maintain zero adjustments on the global mean, which essentially redirects heat from the tropics to the poles.

Because the sea ice coverage decreases in a double CO_2 scenario, these continual, or “on-the-fly” adjustments, redirect less heat from the tropics to the poles, which amounts to an additional climate forcing as shown in Fig. 1 in a zonal mean. Even though the global average of this climate forcing is nearly zero, it influences climate sensitivity because climate feedbacks are not spatially uniform (see, e.g., Boer and Yu 2003b).

Another consideration is that CCSM3-OLDSOM does not account for the latent heat of snow falling into the ocean. (The latent heat of snow that falls on land or sea ice is treated correctly.) In contrast, the atmosphere does

gain heat when ice condensate is formed. In a climate perturbation experiment, the amount of ice condensate produced changes compared to the control, and therefore the energy imbalance is different. In the case of doubling CO_2 , less condensate is produced, resulting in a negative climate forcing of 0.1 W m^{-2} on the global mean, with much higher magnitude locally in the high latitudes of the Southern Hemisphere (see Fig. 1). The extent to which these unphysical climate forcings from on-the-fly adjustments and the latent heat of snow affect the climate and ECS in the CCSM3-OLDSOM is discussed in sections 2d and 3b.

c. Experimental details

To investigate ECS we compare integrations at $1 \times \text{CO}_2$ and $2 \times \text{CO}_2$ levels. The baseline CO_2 level, however, is not the same in CCSM3 and CCSM4. The CCSM3 was developed to produce a long control integration using greenhouse gas and aerosol levels appropriate for the 1990s, and thus its CO_2 concentration is 355 ppmv. As a result the $1 \times \text{CO}_2$ integrations with CCSM3 with a SOM also had a 1990s baseline climate. In contrast, CCSM4 was developed to produce a long control integration of the preindustrial climate with CO_2 concentration at 285 ppmv, which is also used as the baseline for ECS estimates of CCSM4.

Our analysis of SOM integrations use years 31–60, unless otherwise noted. We analyze two idealized CO_2 forcing scenarios with OGCMs. One has a $1\% \text{ yr}^{-1}$ rate of CO_2 increase applied to a branch of a long control integration. In these integrations CO_2 is stabilized once it reaches twice its starting value, which occurs 70 years after CO_2 ramping is initiated. In this case, we analyze 30-yr means centered on the time of doubling. The second type of idealized CO_2 forcing is an instantaneous doubling of CO_2 in the climate model with an OGCM, for which we analyze the whole integration. These idealized scenarios with OGCMs are compared to long control integrations with annually periodic forcing only. We use 30-yr averages from the long controls at a minimum of 400 years from the start of the integration.

Integrations with the CCSM4 atmosphere component at 2° or finer resolution employ a finite volume dynamical core, and therefore the resolution is measured in degrees for the atmosphere and land. The lowest resolution (T31) CCSM4 runs and all integrations with CCSM3 have a spectral dynamical core in the atmosphere, and the land model has the same grid as the atmosphere physics. The ocean and sea ice resolution is nominally 1° when combined with 1° , 2° , T42, or T85 atmospheric resolutions and nominally 3° when combined with T31 atmospheric resolution. For simplicity we note just the resolution of the atmosphere in our presentation.

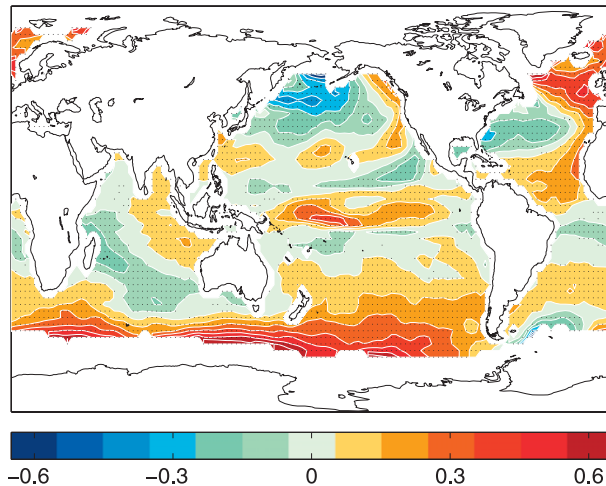


FIG. 2. Sea surface temperature in CCSM3-NEWSOM T42 integration (average of 125 years) minus the climatological SST from CCSM3-OGCM (the target) used to construct the Q_{fix} in $^{\circ}\text{C}$. Gridded dots show grid cells where the SST biases are significantly different from the target, using a 95% (two-sided) confidence interval for a 125-yr run taking account of autocorrelation in the estimate of degrees of freedom in the Student's t distribution.

We assume the radiative forcing from doubling CO_2 is the same in both models and equal to 3.5 W m^{-2} globally averaged, using an estimate from Kay et al. (2012) of the instantaneous tropopause radiative flux change from doubling CO_2 with stratospheric temperatures adjusted to their new thermal equilibrium for CCSM4. Using the same estimate for CCSM3 is partly justifiable given that the radiation code is the same. However, there is an unknown influence from differences in the mean climate state, which we effectively ignore. The estimate of global mean radiative forcing is only a factor in calculating net feedback (see section 3a) and effective climate sensitivity (see section 4).

d. Surface climate in the slab-ocean models

Here we evaluate the influence of the slab-ocean formulation on the surface climatology of the $1 \times \text{CO}_2$ climate. The OLDSOM has not been implemented in CCSM4; therefore, we discuss runs with OLDSOM and NEWSOM in the CCSM3 only.

Both SOMs reproduce the SST and sea ice extent that they are intended to reproduce. Figure 2 shows an example of the SST biases for CCSM3-NEWSOM. Though statistically significant in most regions, the SST biases are typically less than 0.15°C . However, near the sea ice edge, while the CCSM3-NEWSOM biases remain under 0.65°C , in CCSM3-OLDSOM biases reach 2°C (not shown). Arctic sea ice thickness in CCSM3-OLDSOM does not agree well with the limited observations that are available (see Figs. 3a and b), even when accounting

for the difference in time period of model and observation averages. It is much too thick in the central Arctic despite the on-the-fly corrections to the Q_{fix} . Observations are lacking in the Antarctic for comparison, but the overall pattern in the CCSM3-OLDSOM is probably reasonable (not shown). In contrast, the CCSM3-NEWSOM sea ice thicknesses (e.g., Fig. 3c) agree within a half meter of their intended targets (sea ice thicknesses from CCSM3-OGCM, e.g., Figs. 3d) in both hemispheres, except near the Antarctic continent, where the CCSM3-NEWSOM sea ice tends to be thicker than the CCSM3-OGCM sea ice by about a meter (not shown).

3. Climate sensitivity and feedback analysis at equilibrium

The ECS of the CCSM4-NEWSOM is $\Delta T_{\text{eq}} = 2.93^{\circ}\text{C}$ at T31 resolution, 3.13°C at 2° resolution, and 3.20°C at 1° resolution. The ECS of the CCSM4-NEWSOM is higher than that of CCSM3-OLDSOM by about 0.5°C – 0.6°C (see Table 2), when comparing integrations of comparable resolution. This is an increase of roughly 20%. The ECS of CCSM4-NEWSOM differs from CCSM3-NEWSOM by a smaller amount, about 0.35°C . The uncertainties of the ECS in CCSM3-NEWSOM and CCSM3-OLDSOM at T42 resolution are estimated to be 0.07°C (see footnote of Table 2), and we shall assume this is a good approximation for all of our integrations. Given this assumption, ECS is significantly higher in CCSM4-NEWSOM than in both CCSM3-NEWSOM and CCSM3-OLDSOM at every resolution. The resolution of CCSM4-NEWSOM and CCSM3-NEWSOM has no significant influence on ECS above 2° or T42 resolution, while resolution has a modest effect below. This is a smaller effect than the resolution dependence of CCSM3-OLDSOM that was found by Kiehl et al. (2006).

In section 3a we examine the spatial structure of the equilibrium climate response along with a feedback analysis. Then in sections 3b and 3c, we present results from a series of integrations that isolate particular processes to identify the aspects of the models that explain the differences in ΔT_{eq} among the integrations listed in Table 2.

a. Climate sensitivity and feedback analysis of CCSM3 versus CCSM4

We now present a more detailed analysis of the causes for variations in the spatial and global equilibrium responses in our three main configurations, each at the highest resolution: CCSM3-OLDSOM T85, CCSM3-NEWSOM T85, and CCSM4-NEWSOM 1° . The zonal-mean equilibrium surface air temperature change from

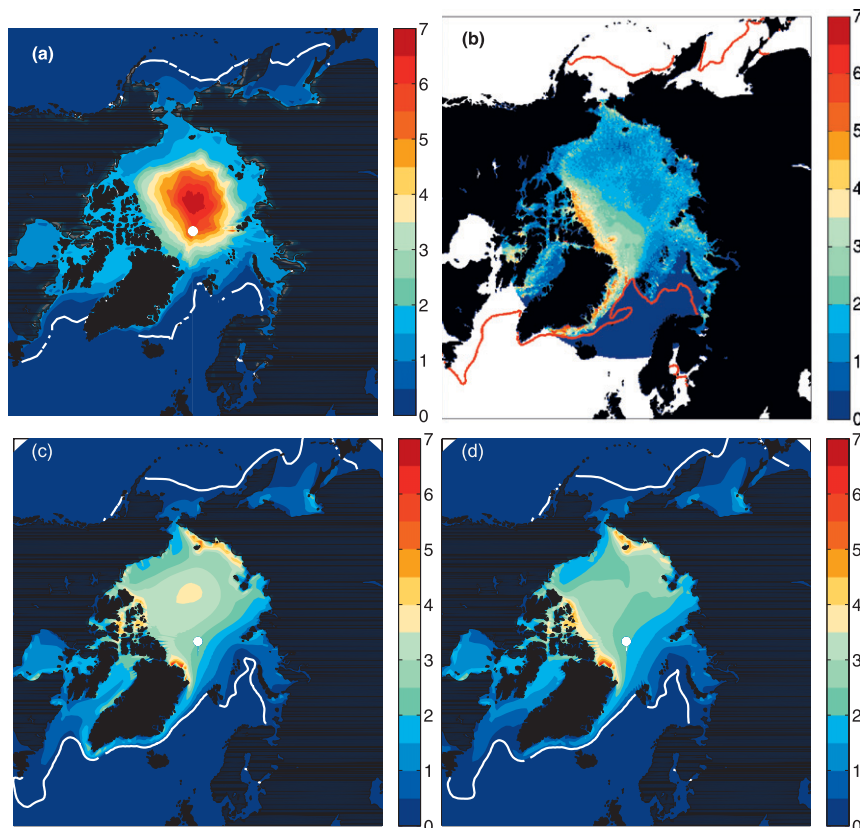


FIG. 3. Arctic March sea ice thickness in meters and extent as defined by the 15% ice concentration contour in (a) OLD SOM-CCSM3 T85, (b) observations, (c) NEWSOM-CCSM3 T85, and (d) CCSM3-OGCM T85 1990s control. Observations of sea ice thickness are based on ICESat laser altimeter (Yi and Zwally 2010) for which only 2006 and 2007 are available. Observations of ice concentration are from NASA passive microwave (Comiso 1990). All integrations here have 1990s-level greenhouse gas forcing. It is possible that the true ice thickness was ~ 1 m greater in 1990 compared to what is shown here.

these integrations is shown in Fig. 4a. CCSM4-NEWSOM warms more than both CCSM3-OLDSOM and CCSM3-NEWSOM at the surface at every latitude, except just at the equator. There is an unusual small local warming maximum on the equator in CCSM3-OLDSOM that is comparably smaller in the CCSM3-NEWSOM and does not occur at all in the CCSM4-NEWSOM (see Fig. 4a).

The temperature change aloft does not necessarily follow these surface air temperature and lower-troposphere changes. Instead CCSM4-NEWSOM warms the least above about 300 hPa between 30°S and 30°N , as seen in vertical temperature profile averages (see Fig. 4c). CCSM3-OLDSOM generally warms the most above 700 hPa in the 30°S – 30°N average, even though its zonal-mean warming is the least at the surface at nearly every latitude. CCSM4-NEWSOM's decreased temperature change with height, combined with the increased temperature change in the lower troposphere, indicates a different lapse rate response for CCSM4-NEWSOM in addition

to the different meridional temperature gradient response, with CCSM3-NEWSOM generally having a temperature response magnitude between those of the other two configurations.

Accordingly, the upper-tropospheric water vapor in CCSM4 also increases the least (see Fig. 5), especially in the tropics and subtropics. Below 500 hPa, CCSM4-NEWSOM tends to moisten as much or more than CCSM3-OLDSOM and CCSM3-NEWSOM, partially compensating for the decreased water vapor change of CCSM4-NEWSOM higher in the troposphere. The larger temperature changes combined with the smaller water vapor changes between 600 and 700 hPa result in roughly a 1% reduction in relative humidity in the tropics at that level for both CCSM3-OLDSOM and CCSM3-NEWSOM that does not occur in CCSM4-NEWSOM (not shown).

Middle- to high-level cloud fractions at the equator increase in CCSM3-OLDSOM (see Fig. 6a) but there is

TABLE 2. Equilibrium climate sensitivity for standard versions of the models.

Model version and SOM method	Resolution	$\Delta T_{\text{eq}}^{\text{a}}$ °C
CCSM3-OLDSOM	T31	2.40 ^b
CCSM3-OLDSOM	T42	2.53 ^b \pm 0.07 ^c
CCSM3-OLDSOM	T85	2.71
CCSM3-NEWSOM	T31	2.47
CCSM3-NEWSOM	T42	2.80 \pm 0.07 ^c
CCSM3-NEWSOM	T85	2.86
CCSM4-NEWSOM	T31	2.93
CCSM4-NEWSOM	2°	3.13
CCSM4-NEWSOM	1°	3.20

^a The global mean in all runs is the mean of years 31–60, except in CCSM3-OLDSOM T31 and T85, where it is from years 31–50.

^b These values may differ slightly from Kiehl et al. (2006) because we use longer averaging periods.

^c Uncertainties are $2\sqrt{2}\sigma$, where σ is the standard deviation of 30-yr intervals in 210-yr-long runs at $1 \times \text{CO}_2$. The 30-yr intervals are nonoverlapping in years 1–210 and additionally 16–195 (for a total of 13 intervals). The potential bias from not reaching a true equilibrium by year 31 is estimated to be less than 0.01°C based on extending the $2 \times \text{CO}_2$ integrations to 110 years.

little change in CCSM3-NEWSOM and even a reduction in CCSM4-NEWSOM. These cloud changes are consistent with the local surface air temperature changes at the equator. From 10° to 20°N and 10° to 20°S the middle- to high-level cloud fractions change with opposite sign to the equatorial values, again with CCSM3-OLDSOM changing the most and CCSM4-NEWSOM changing the least. We also examined the cloud fraction changes in two-dimensional maps and in the three runs shown in Fig. 6 and in some of our sensitivity experiments (not shown). These additional analyses suggest the primary reason for the tropical cloud differences is mean state SST between CCSM3-NEWSOM and CCSM3-OLDSOM and the new turbulence closure scheme in the convective clouds in CCSM4-NEWSOM.

Poleward of about 60° north or south, cloud fraction increases at all levels in all models (see Fig. 6). Low cloud fraction increases considerably more in CCSM4-NEWSOM than in both CCSM3-NEWSOM and CCSM3-OLDSOM in the polar regions. The polar low cloud increase in CCSM4-NEWSOM is primarily from the new freeze-dry parameterization (based on analysis of our sensitivity experiments). In contrast, there is a reduction in low clouds from 40° to 55°S in all models, but it is about twice as large in CCSM4-NEWSOM compared with CCSM3-OLDSOM and CCSM3-NEWSOM.

To interpret these and other changes and determine their effects on the climate sensitivity, we use climate feedback analysis. The underlying assumption is that the global surface air temperature responds to an imposed

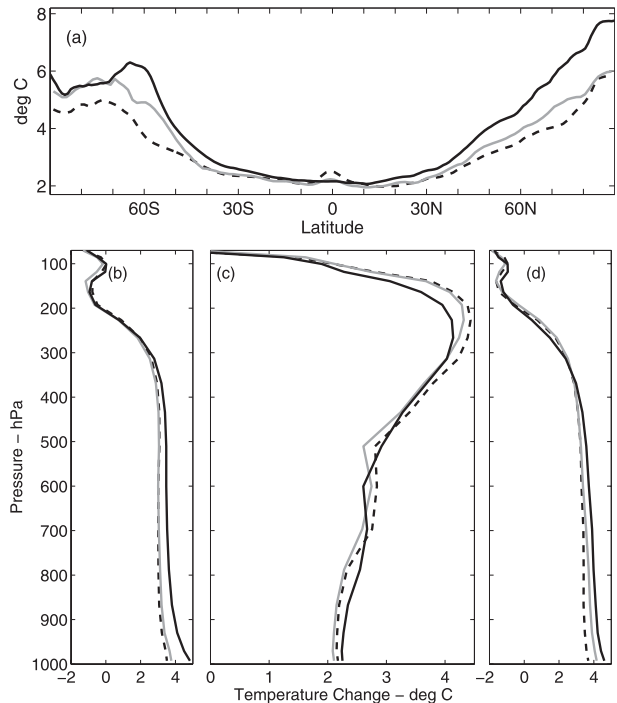


FIG. 4. (a) Change in zonal mean surface air temperature and vertical temperature profiles (b) south of 30°S, (c) 30°S–30°N, and (d) north of 30°N from doubling CO_2 in CCSM4-NEWSOM 1° (solid black), CCSM3 NEWSOM T85 (solid gray), and CCSM3-OLDSOM T85 (dashed black).

top of atmosphere (TOA) radiative forcing, and then feedbacks arise in response to the surface air temperature change to further alter the TOA budget. At any given point in time, the radiative imbalance at the TOA is the sum of the TOA radiative forcing ΔR_f and the TOA flux changes (feedback) due to changes in the global surface air temperature. The radiative kernel feedback method (Soden and Held 2006; Soden et al. 2008) assumes that these feedback flux changes are linear with respect to the global annual average surface air temperature change ΔT :

$$\Delta R = \Delta R_f + \lambda \Delta T, \quad (2)$$

where λ is the net feedback parameter, and $\Delta R = \Delta Q - \Delta F$ is the change in absorbed shortwave radiation minus the change in outgoing longwave radiation at the TOA due to both the imposed forcing and the climate response (i.e., feedbacks). Here we have chosen the sign convention that positive λ indicates a positive feedback (enhances climate changes). For the kernel feedback method, ΔR , ΔR_f , and λ may vary spatially, but ΔT is always averaged globally. Thus λ can be viewed as an efficiency of fluxing heat out the TOA for a given global mean temperature change.

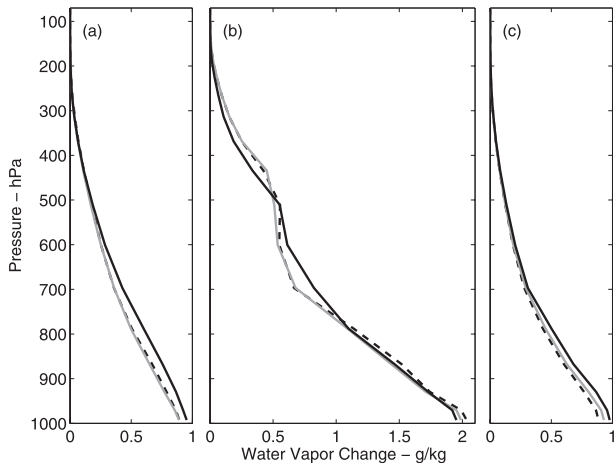


FIG. 5. As in Fig. 4b, but for humidity profiles.

The kernel method separates climate feedbacks into different components:

$$\lambda = \lambda_P + \lambda_{LR} + \lambda_w + \lambda_\alpha + \lambda_c + r, \quad (3)$$

where λ_P is the Planck feedback, λ_{LR} is the lapse-rate feedback, λ_w is the water vapor feedback, λ_α is the surface albedo feedback, λ_c is the cloud feedback, and r is a residual that results from the nonlinear contributions to the feedback parameter or other radiative elements that are not included in the decomposition. We assume that the Planck, lapse-rate, water vapor, and surface albedo feedback parameters are independent of the climate state (at least for the range of states simulated here), and we calculate these feedbacks by combining the changes in these quantities in the double CO_2 experiments with the precalculated radiative kernels of Shell et al. (2008). We use the adjusted cloud radiative forcing to estimate cloud feedback following Soden et al. (2008). The cloud component can be further broken down into shortwave and longwave feedbacks (λ_c^{LW} and λ_c^{SW}) according to their influence on ΔQ and ΔF separately. The same is true for λ_w ; however, the shortwave component of the water vapor feedback is nearly always the same so the longwave component accounts for most of the range in λ_w .

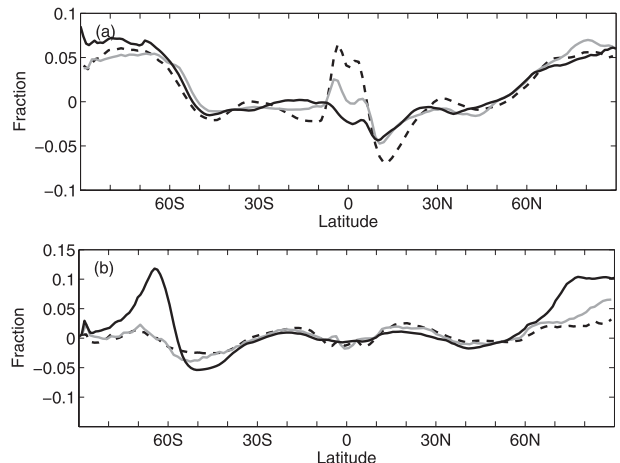


FIG. 6. As in Fig. 4a, but for (a) mid to high clouds and (b) low clouds.

Table 3 lists the global annual mean net feedbacks and their components. The strong negative Planck feedback is relatively similar among the models, as expected. The (negative) lapse-rate feedback varies the most among the different model versions, with a steady decrease from CCSM3-OLDSOM to CCSM3-NEWSOM to CCSM4-NEWSOM, while the (positive) water vapor feedback decreases, partially compensating for the lapse rate feedback decrease. The global average albedo feedback changes little.

Net cloud feedback decreases from CCSM3-OLDSOM to CCSM3-NEWSOM, and then increases from CCSM3-NEWSOM to CCSM4-NEWSOM, resulting in little change from CCSM3-OLDSOM to CCSM4-NEWSOM; however, the longwave and shortwave cloud feedbacks, which are both positive, change slightly more. In CCSM3-OLDSOM, the positive cloud feedback was primarily due to the cloud longwave radiative response (Shell et al. 2008), while in CCSM4-NEWSOM, the shortwave and longwave radiative responses are about equal in magnitude.

Global-average feedback values are often the result of compensation between regions of positive and negative feedbacks (especially for the lapse-rate and cloud feedbacks). Since the global mean values can hide some of the regional changes in feedbacks parameters, it is useful to consider the spatial feedback pattern.

TABLE 3. Global annual mean climate feedbacks in $\text{W m}^{-2} \text{K}^{-1}$ from kernel method.

Model version	λ^*	λ_P	λ_{LR}	λ_w	λ_α	λ_c	λ_c^{LW}	λ_c^{SW}
CCSM3-OLDSOM T85	-1.37	-3.05	-0.42	1.62	0.32	0.46	0.36	0.11
CCSM3-NEWSOM T85	-1.30	-3.00	-0.25	1.50	0.34	0.38	0.28	0.10
CCSM4-NEWSOM 1°	-1.16	-2.98	-0.10	1.43	0.32	0.48	0.23	0.25

* The net λ is computed from Eq. (2) using $\Delta R_f = 3.5 \text{ W m}^{-2}$ (discussed in section 2).

The sign of the regional lapse-rate feedback (Fig. 7) is generally the same for all the models, except in the eastern tropical Pacific, but the magnitudes of the regional feedbacks differ among models. The lapse-rate feedback is most negative (results in the most outgoing longwave radiation increase with increasing temperature) where the lapse rate decreases the most in the doubling CO_2 experiment. Figure 4b shows that CCSM3-OLDSOM has the largest temperature change in the tropical upper troposphere (corresponding to the largest lapse rate decrease), so the CCSM3-OLDSOM has the most negative tropical lapse-rate feedback, except on the equator in the eastern tropical Pacific. CCSM4-NEWSOM, conversely, has the weakest negative tropical lapse rate feedback. At middle and high latitudes, all models show a transition to a positive lapse-rate feedback, with CCSM4-NEWSOM having the largest positive lapse-rate feedback and CCSM3-OLDSOM the smallest. Thus, CCSM4-NEWSOM is generally more positive regionally compared with the other models, so the global average lapse-rate feedback, while still negative, is small, while CCSM3-OLDSOM has the largest global average feedback.

The lapse-rate feedback variations in the tropics among the model versions are roughly opposite to their water vapor feedback variations, except in the eastern tropical Pacific. For example, in the tropics CCSM4-NEWSOM has the least negative lapse-rate feedback and the least positive water-vapor feedback. This partial compensation is expected because the relative humidity changes little when CO_2 is doubled; however, the global average feedback differences among models are larger for the lapse-rate than water vapor feedbacks, so the net effect is an increase in climate sensitivity from CCSM3-OLDSOM to CCSM3-NEWSOM to CCSM4-NEWSOM.

Kiehl et al. (2006) reported that the CCSM3-OLDSOM at T85 resolution overpredicts clouds in the lowest model level in the eastern tropical Pacific at $1 \times \text{CO}_2$ but not at $2 \times \text{CO}_2$. It is in this region that the lapse-rate feedback is strongly positive in CCSM3-OLDSOM. There is only slight evidence for this problem in the CCSM3-NEWSOM at T85 resolution, and therefore the differing mean state SST or the unphysical forcings in the OLDSOM must exacerbate the problem. The problem is not present in CCSM4 at any resolution or model configuration.

Aside from the eastern tropical Pacific, shortwave and longwave cloud feedbacks have opposite signs for a given model version. Local maxima and minima tend to be larger in magnitude in CCSM3-OLDSOM. Shortwave cloud feedback especially is more homogeneous in CCSM4-NEWSOM compared to CCSM3-OLDSOM

and even CCSM3-NEWSOM (see Fig. 8), except it retains a consistent positive, high magnitude in the mid-latitudes of the Southern Hemisphere. In this region, Fig. 6 indicates low clouds decline sharply when CO_2 is doubled in CCSM4-NEWSOM. This region is equatorward of the sea ice zone, and therefore the cloud decrease does little to amplify sea ice albedo feedback here. However, at the poles, low clouds expand considerably in CCSM4-NEWSOM and mask the sea ice retreat from the TOA perspective.

The pattern of longwave cloud feedback in CCSM4-NEWSOM is also more homogeneous than in CCSM3-NEWSOM, which in turn is more homogeneous than in CCSM3-OLDSOM. The region of strong negative longwave cloud feedback in the tropical Pacific and near Indonesia present in CCSM3-OLDSOM is gone in CCSM4-NEWSOM. These are regions where medium and high clouds decrease in CCSM3-OLDSOM but change little in CCSM4-NEWSOM when CO_2 is doubled.

b. Dependence on the SOM formulation

The ECS differs by as much as 0.27°C depending on the SOM formulation (i.e., comparing CCSM3-NEWSOM and CCSM3-OLDSOM at the same resolution). This is roughly half the difference between CCSM3-OLDSOM and CCSM4-NEWSOM at similar resolutions. There are three issues that might affect the climate response with regard to the SOM formulation: one is the influence of the unphysical forcings in the OLDSOM (see Fig. 1), the second is the influence of differences in the mean state of the climate, and the third is the differences in sea ice physics. Numerous studies have shown that the climate response depends on the horizontal structure of climate forcings (e.g., Hansen et al. 1997), while only a few have found a small (10%–20% change in effective climate sensitivity) dependence on climate state (e.g., Senior and Mitchell 2000; Boer and Yu 2003a) or sea ice physics (e.g., Holland et al. 2001).

The net feedback in CCSM3 is generally higher in the polar regions, owing to the ice-albedo and lapse-rate feedback (see section 3a), precisely where both unphysical climate forcings in the OLDSOM are sharply negative. Thus, we might expect the unphysical forcings to inhibit feedback, and, hence, the climate sensitivity. We ran sensitivity experiments with the CCSM3 to evaluate the consequences of both unphysical forcings (see Table 4).

We eliminated the unphysical forcings in $1 \times \text{CO}_2$ and $2 \times \text{CO}_2$ sensitivity experiments in the CCSM3-OLDSOM by taking into account the latent heat of snow falling into the ocean, while simultaneously fixing the on-the-fly adjustments (so they are not on-the-fly anymore) to the Q_{fix} .

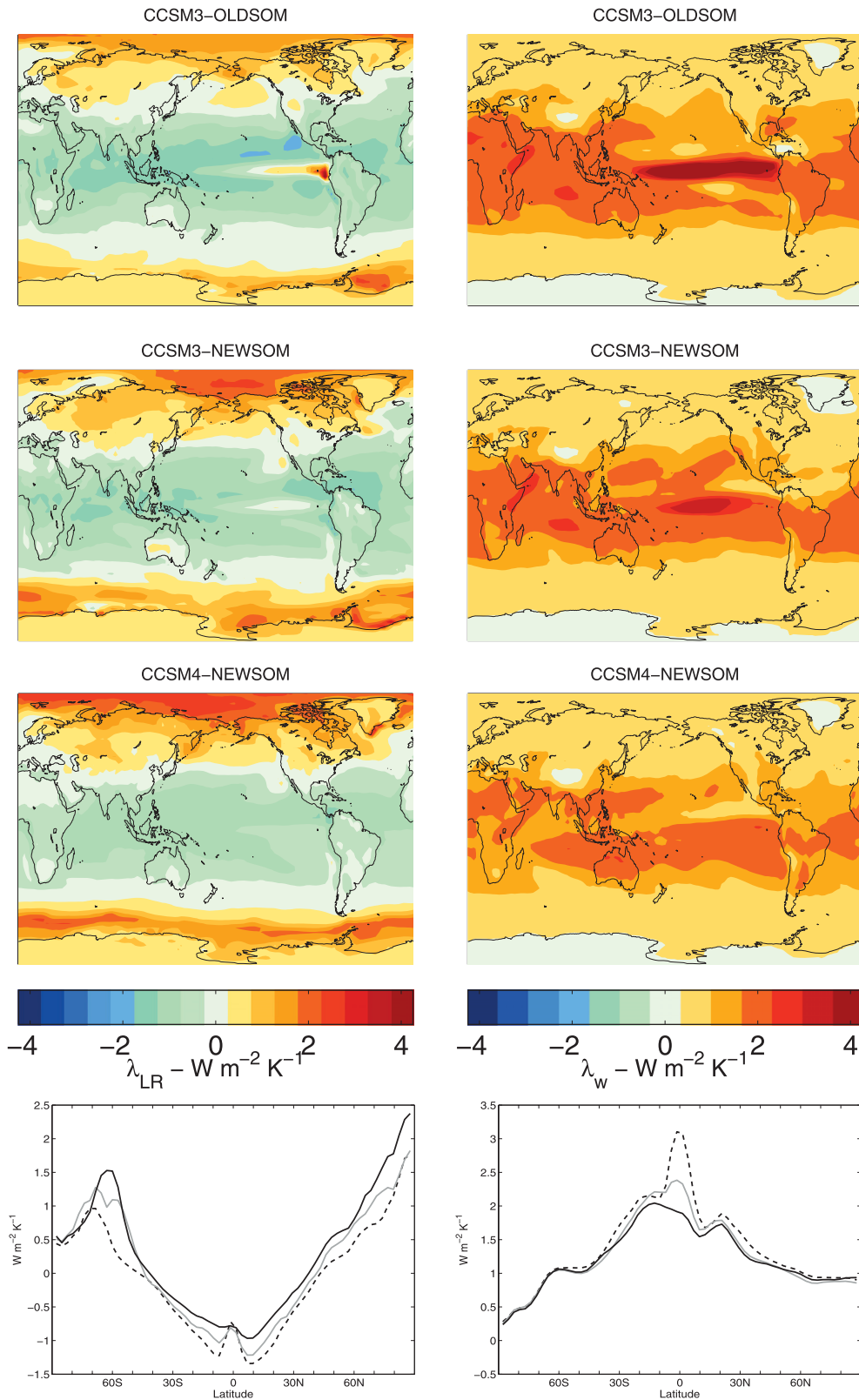


FIG. 7. (left) Feedbacks from the kernel method for lapse rate and (right) longwave water vapor in $\text{W m}^{-2} \text{K}^{-1}$: (top) CCSM3-OLDSOM, (next row) CCSM3-NEWSOM, and (next to bottom) CCSM4-NEWSOM. (bottom) Line colors for zonal mean plots as in Fig. 4.

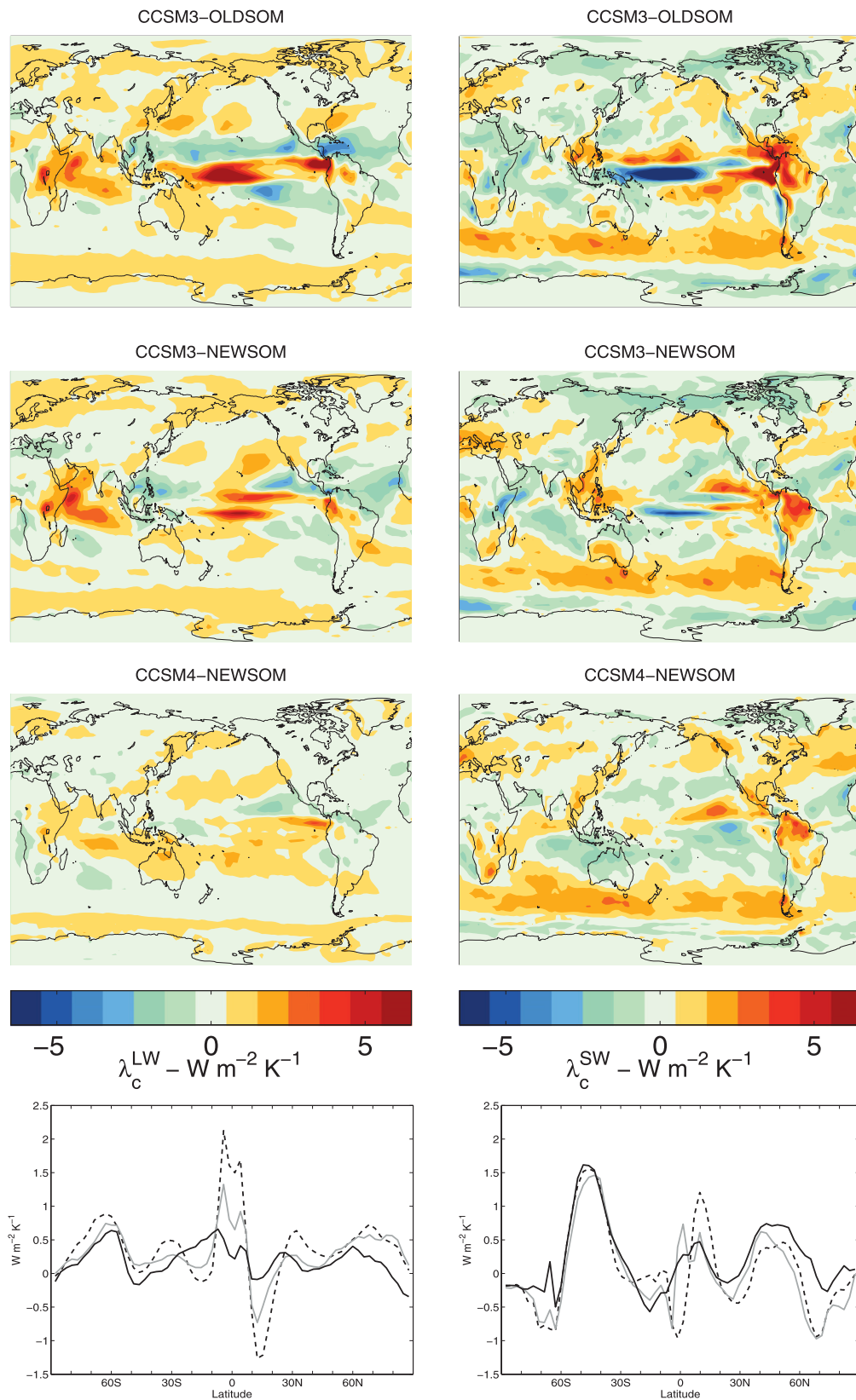


FIG. 8. As in Fig. 7, but for longwave cloud and shortwave cloud in $W m^{-2} K^{-1}$.

TABLE 4. Equilibrium climate sensitivity in a series of runs with altered slab-ocean model physics in CCSM3 OLDSOM.

ΔT_{eq} in $^{\circ}\text{C}$	Run description
2.53	T42, original run with standard physics, which has on-the-fly adjustment to Q_{fix} and does not account for latent heat of snow falling into ocean
2.79	T42, eliminating the unphysical forcing from just the on-the-fly adjustment to Q_{fix}
3.00	T42, eliminating the unphysical forcing from both the latent heat of snow falling into ocean and the on-the-fly adjustment to Q_{fix}
2.71	T85, original run with standard physics, which has on-the-fly adjustment to Q_{fix} and does not account for latent heat of snow falling into ocean
3.21	T85, eliminating the unphysical forcing from both the latent heat of snow falling into ocean and the on-the-fly adjustment to Q_{fix}

We did this by first extracting the climatological mean of the on-the-fly adjustments from the original $1 \times \text{CO}_2$ run of Kiehl et al. (2006). We then increased the Q_{fix} that is normally used as input to CCSM3-OLDSOM by the climatology of the on-the-fly adjustments along with the latent heat of the climatological mean rate of snow falling into the ocean from the original $1 \times \text{CO}_2$ run. Finally, this modified Q_{fix} was input to the CCSM3-OLDSOM with minor code changes to account for snowfall in F_{net} and eliminate the on-the-fly adjustments. The resulting sensitivity experiment at $1 \times \text{CO}_2$ by construction produces an SST and mean climate that is not significantly different from the original $1 \times \text{CO}_2$ run. However, when CO_2 is doubled, ECS is 0.47°C higher at T42 resolution and 0.50°C higher at T85 resolution in the sensitivity experiments compared to the original $2 \times \text{CO}_2$ runs. The zonal mean surface warming increases at all latitudes in the Southern Hemisphere (see Fig. 9), especially in the high southern latitudes. The increase is also large in the Arctic. The regions of greatest increase in surface warming coincide with the regions where the unphysical forcings are most negative in the original OLDSOM (see Fig. 1).

Another pair of sensitivity experiments was done at T42 resolution eliminating only the unphysical forcing from the on-the-fly Q_{fix} adjustments compared to the original runs, and in this case ECS is 0.26°C higher. We did not do this test at T85 resolution.

In summary we find that the energy sources and sinks created by the on-the-fly adjustments to the Q_{fix} and neglecting the latent heat of snow cause unphysical forcings in the CCSM3-OLDSOM that suppress the estimated ECS by about 0.5°C . Because the unphysical forcings are nearly the same at T42 (not shown) and T85 resolutions (see Fig. 1), the suppressed amount is nearly

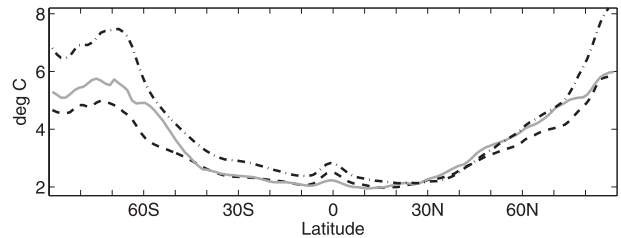


FIG. 9. Zonal mean surface air temperature change from doubling CO_2 in CCSM3-NEWSOM T85 (solid gray), CCSM3-OLDSOM T85 (dashed black), and CCSM3-OLDSOM T85 with both unphysical forcings eliminated (dot-dashed black).

independent of resolution. The CCSM3-NEWSOM has neither unphysical forcing, yet the ECS of CCSM3-NEWSOM is about 10% smaller than in CCSM3-OLDSOM with the unphysical forcing eliminated (see Fig. 9). The climate response differs owing purely to differences in the mean state climate (via differences in SST and sea ice climatology in the SOMs) and/or sea ice physics.

c. Sensitivity tests of new physics and parameters in CCSM4

Next we investigate the influence of new CCSM4 physics parameterizations and the mean state climate on climate sensitivity in CCSM4 compared to CCSM3. The sensitivity experiments described in this section are done with the NEWSOM using the Q_{fix} constructed from a long control with the OGCM with standard physics and forcing in all components. Unfortunately, the best estimate of ECS would require a new Q_{fix} for each sensitivity experiment based on a new long control with the perturbed physics–forcing. This is impractical. Our failure to recalibrate the Q_{fix} neglects changes to the ocean heat transport (and thus the Q_{fix}), which might affect the mean climate state. Thus changes to the sensitivity of ECS to perturbed physics–forcing quoted in this section are subject to the caveat that they do not include changes to the Q_{fix} . In the remainder of this section we refer to results that are exclusively from the NEWSOM, and thus we drop the term from the model version names.

One might guess that the greater high-latitude warming in CCSM4 could be a result of the preindustrial baseline climate in CCSM4, as compared to the present-day baseline climate in CCSM3. The expanded sea ice and snow in the preindustrial climate could yield a greater ice–albedo feedback. However, studies have shown this to be a small or even negligible effect in the past (Rind et al. 1997; Holland and Bitz 2003). We tested the effect nonetheless by raising CO_2 to year 2000 level

(at 379 ppmv) in a $1 \times \text{CO}_2$ baseline CCSM4 simulation and doubling the CO_2 concentration from there. This raises ΔT_{eq} in CCSM4 by 0.16°C compared to the standard runs (see Table 5), indicating an increase rather than decrease in climate sensitivity for a warmer base climate. Thus the higher ECS in CCSM4 cannot be explained by the colder preindustrial baseline climate in CCSM4 compared to the warmer baseline climate in CCSM3. We thus consider other CCSM4 changes as possibilities for the increase in CCSM4 sensitivity.

One significant change in CCSM4 is the freeze-dry cloud parameterization (see the model description in section 2). We tested its influence on CCSM4 climate change by conducting sensitivity experiments at $1 \times \text{CO}_2$ and $2 \times \text{CO}_2$ with the parameterization eliminated. The primary effect of the freeze-dry parameterization is to reduce low cloud fraction by about 10%–20% in the polar regions in the $1 \times \text{CO}_2$ climate. The effect is diminished at $2 \times \text{CO}_2$, and therefore including this parameterization in CCSM4 causes a large increase in low cloud amount in the polar regions when CO_2 is doubled. Without this parameterization, the polar regions warm about 0.5°C more and ΔT_{eq} is 0.22°C higher (Table 5). Thus, its inclusion in CCSM4 reduces ECS and masks other factors that raise ECS in CCSM4 compared to CCSM3.

We were able to identify one parameterization change that does increase ECS in CCSM4. It involves how snow buries vegetation when it accumulates at the surface. We performed a doubled CO_2 experiment with a version of CCSM4 with the old CCSM3 snow burial parameterization, resulting in a decreased ECS. Thus, the new parameterization in CCSM4 increases ECS by 0.20°C . Despite the increased sensitivity from this parameterization change, we found no increase to the global mean surface albedo feedback in CCSM4 compared to CCSM3 (see Table 3). There must be a compensating change to the surface albedo parameterization that cancels the effects from the snow burial changes on the whole.

In total, our attempt at explaining the higher ECS in CCSM4 compared to CCSM3 through sensitivity experiments revealed no single major cause. Lowering the baseline CO_2 in CCSM4, lowers ECS slightly, all other things being equal. The new freeze-dry cloud parameterization also lowers ECS. Among the parameters/forcings we isolated in this section, we found only the new snow burial rate parameterization raises ECS, but it is only a partial explanation for the differences between CCSM4 and CCSM3. The diagnostic analysis of section 3a identified changes in deep convection as a major factor in altering lapse-rate, water vapor, and cloud feedbacks, but we did not do sensitivity experiments to isolate effects from the new deep convection parameterization on ECS.

TABLE 5. Equilibrium climate sensitivity in series of runs with varying physics and parameters in CCSM4-NEWSOM.

ΔT_{eq} in $^\circ\text{C}$	Run description*
3.13	2° standard physics
3.20	1° standard physics
3.36	1° standard physics but with year 2000 CO_2 concentration baseline
3.35	2° standard physics except without CCSM4's new cloud freeze-dry parameterization (Vavrus and Waliser 2008)
3.00	1° standard physics except revert to vegetation snow burial method from CCSM3

* In each case the q_{flux} is from a preindustrial CCSM4 OGCM run at the same resolution as the integration to which it is prescribed.

4. Transient versus equilibrium climate sensitivity and the role of ocean dynamics

Because the NEWSOM reproduces the OGCM's SST and sea ice cover, transient and equilibrium perturbation experiments can be compared consistently between runs with NEWSOM and OGCM. The climate difference between them cleanly shows the role of ocean dynamics and deep-ocean warming, without being confused by differing states of the SST or sea ice cover and sea ice physics. In this section we compare the climate response of CCSM3 and CCSM4 to doubling CO_2 in transient integrations (with OGCM) and equilibrium integrations (with NEWSOM). We then delve further into the transient behavior of the CCSM4-OGCM for which we have a 309-yr-long integration following an instantaneous CO_2 doubling. All integrations described in this section are at the highest resolution considered in this study (T85 for CCSM3 and 1° for CCSM4).

We first examine the transient behavior of CCSM3-OGCM and CCSM4-OGCM in 1% per year (continuously updated) CO_2 ramp integrations. Standard metrics that characterize the global annual mean transient response at the time of doubling (year 70) are listed in Table 6. The global annual surface air temperature change at the time of CO_2 doubling is known as the transient climate response [TCR, $\Delta T(70 \text{ yr})$]. The effective climate sensitivity at the time of CO_2 doubling [$\Delta T_{\text{eff}}(70 \text{ yr})$], as defined by Murphy (1995), is an estimate of the ECS by extrapolating the TCR to the time when the TOA radiative imbalance goes to zero while assuming climate feedbacks are constant in time and equal to the magnitude at year 70. In practice, the time series $\Delta T_{\text{eff}}(t)$ is equal to $\Delta T(t)$ scaled by $\Delta R_f / [\Delta R_f - \Delta R(t)]$.

The TCR and $\Delta T_{\text{eff}}(70 \text{ yr})$ are both smaller in CCSM3 than in CCSM4. Yet, the global annual mean TOA radiative imbalance [$\Delta R(70 \text{ yr})$] is nearly identical in the models. On the global annual mean the ocean heat uptake, by

TABLE 6. Transient climate response, effective climate sensitivity, and TOA radiative imbalance in 1% CO₂ ramp OGCM runs at time of doubling; equilibrium climate sensitivity from NEWSOM runs; and ratios of transient climate response to equilibrium climate sensitivity and effective climate sensitivity to equilibrium climate sensitivity.

Model version	$\Delta T(70 \text{ yr})$ °C	$\Delta T_{\text{eff}}(70 \text{ yr})$ °C	$\Delta R(70 \text{ yr})$ W m ⁻²	ΔT_{eq} °C	$\frac{\Delta T(70 \text{ yr})}{\Delta T_{\text{eq}}}$	$\frac{\Delta T_{\text{eff}}(70 \text{ yr})}{\Delta T_{\text{eq}}}$
CCSM3 T85	1.54	2.37	1.23	2.86	0.54	0.83
CCSM4 1°	1.72	2.64	1.22	3.20	0.54	0.83

which we mean the surface heat flux into the ocean, is nearly equivalent to ΔR . The greater the ocean heat uptake, the more suppressed the surface warming and the greater the ΔR . Despite the apparent logic of this statement, the amount the surface warming is suppressed is not exclusively a function of ocean heat uptake in cross-model intercomparisons (see, e.g., IPCC 1990). Winton et al. (2010) argues this is because different models respond differently to a given amount of ocean heat uptake. However, our two models do appear to suppress warming about the same amount for a given amount of heat uptake, as $\Delta R(70 \text{ yr})$ and the ratio of TCR to ECS [and of $\Delta T(70 \text{ yr})_{\text{eff}}$ to ECS] is the same for the two models within a percent.

We believe that these ratios in CCSM3 and CCSM4 are nearly the same because not only is their global mean ocean heat uptake nearly the same, but the latitudinal dependence is very similar (see Fig. 10a). The rate of decline in ocean heat uptake is largest in the mid to high latitudes, where warming at equilibrium is greatest (see Fig. 4a) and feedbacks are above average in CCSM3 and CCSM4 (see Fig. 10b). We speculate that the more polar amplified the rate of decline in ocean heat uptake, the smaller the ratios of $\Delta T(t)$ to ΔT_{eq} and ΔT_{eff} to ΔT_{eq} .

We end our analysis of transient climate response in CCSM4-OGCM by examining the time dependent response of a 309-yr integration with CO₂ doubled instantly at the start. The time series of $\Delta T(t)$ (see Fig. 11a) indicates that the global annual mean warming reached at the end (about 2.5°C) is still substantially below the ECS ($\Delta T_{\text{eq}} = 3.20^\circ\text{C}$). Much of this difference arises from greater warming in the NEWSOM compared to the OGCM in the Pacific and Atlantic sectors of the Southern Ocean and just south of Greenland (see Fig. 12), all regions of deep mixing and large ocean heat uptake. The OGCM SST warms more than the NEWSOM in the Barents Sea—a result seen in CCSM3 as well (Bitz et al. 2006).

The time series of $\Delta T_{\text{eff}}(t)$ (see Fig. 11b) is noisier than $\Delta T(t)$. Yet, the smoothed $\Delta T_{\text{eff}}(t)$ is always less than the ECS, and it is unclear if $\Delta T_{\text{eff}}(t)$ is asymptoting to $\Delta T_{\text{eq}}(t)$. The time dependence of $\Delta T_{\text{eff}}(t)$ has been attributed to a time dependence of climate feedbacks (e.g., Senior and Mitchell 2000). Indeed, as defined in Eq. (2), the global mean net λ (not shown) is inversely

proportionate to $\Delta T_{\text{eff}}(t)$, but the time dependence of λ may be an indication that Eq. (2) is not an optimal definition of feedback. We propose that the time dependence of the pattern of ocean heat uptake is possibly a more fundamental factor that affects the time evolution of estimates of climate sensitivity. Ocean heat uptake declines about 50% faster in the mid to high latitudes (averaging in zeros over land) than it does in

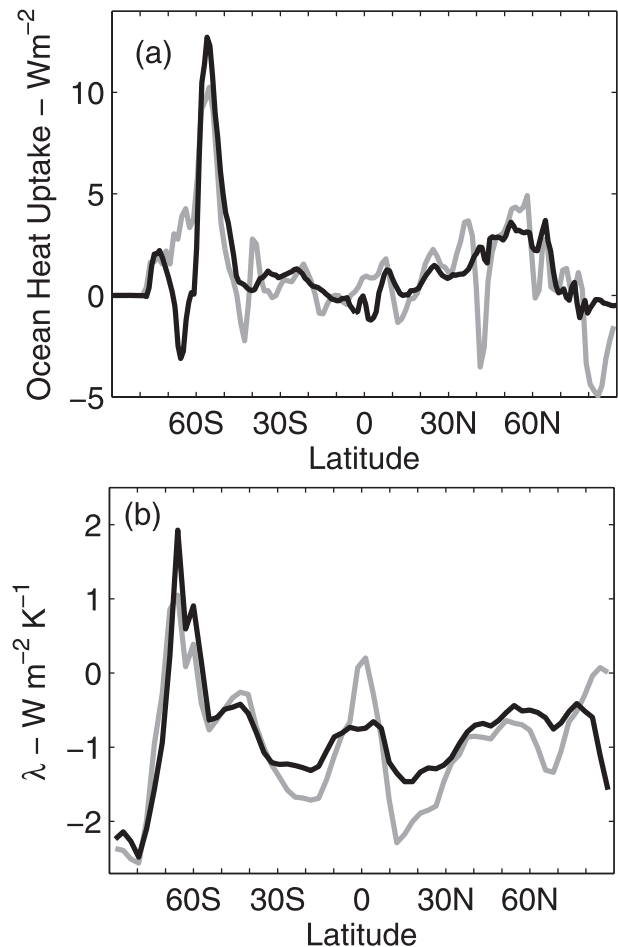


FIG. 10. (a) Zonal mean change in ocean heat uptake in CO₂ ramp runs with OGCM from 30-yr means centered on the time of doubling and (b) zonal mean net feedback λ in equilibrium runs with NEWSOM for CCSM3 (gray) and CCSM4 (black). Zonal mean ocean heat uptake includes zeros over land.

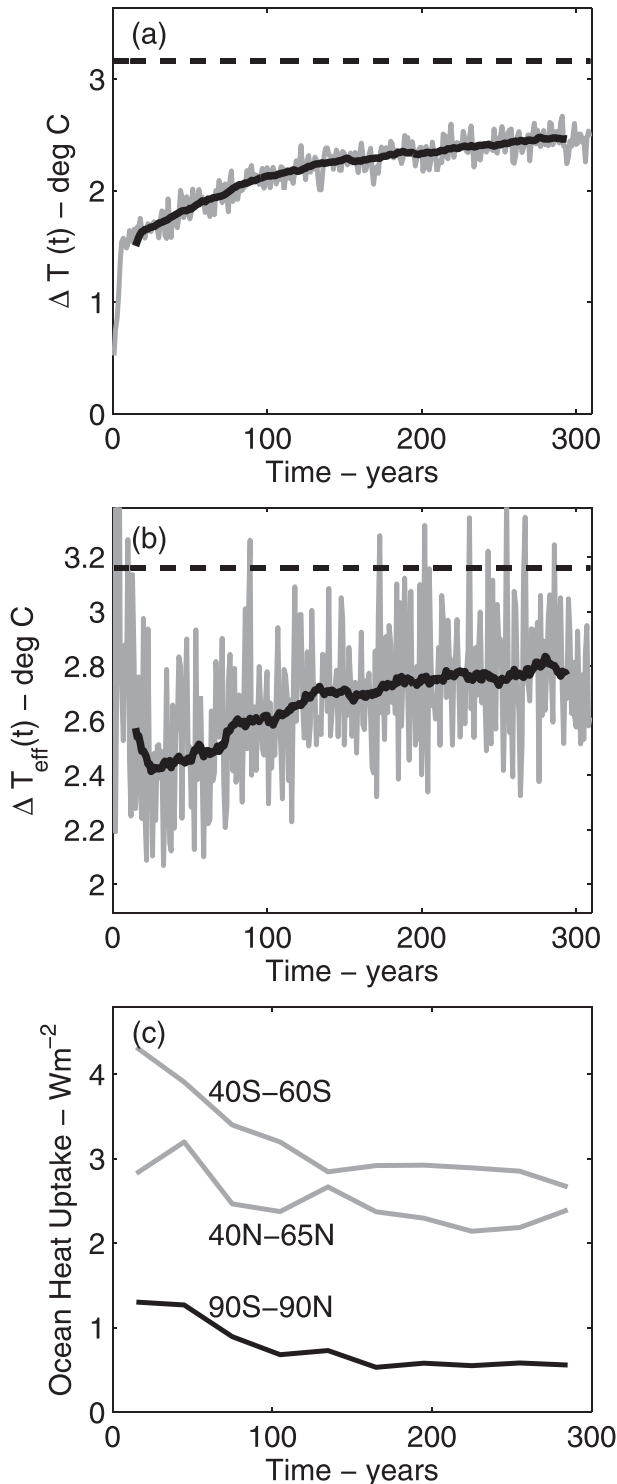


FIG. 11. Time-dependent variables from CCSM4-OGCM integration with CO_2 doubled instantly at year 0: (a) global mean surface air temperature change and (b) effective climate sensitivity, computed annually (gray) and smoothed with a 30-yr running mean (black solid). (c) Ocean heat uptake averaged over latitude ranges as indicated for 30-yr means, including zeros over land. ECS is dashed in (a),(b).

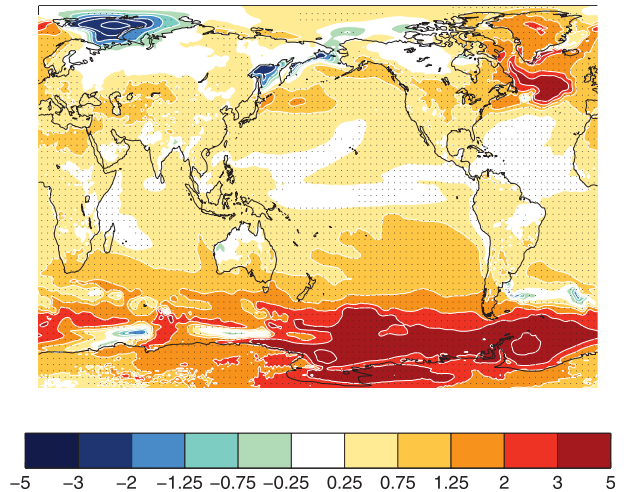


FIG. 12. Surface air temperature change in $^{\circ}\text{C}$ (difference of ΔT 's) from doubling CO_2 , CCSM4-NEWSOM 1° at equilibrium (yr 31–60) minus CCSM4-OGCM 1° after 3 centuries (yr 280–309) in the instant CO_2 doubling experiment. Gridded dots show regions where the surface temperature is significantly different at the 95% confidence interval.

other regions (see Fig. 11c), and therefore, $\Delta T_{\text{eff}}(t)$ should be less suppressed in time. The transient response of $\Delta T_{\text{eff}}(t)$ is roughly in line with the reduction in ocean heat uptake from 40° to 60°S . The ocean heat uptake may never reach zero locally if doubling CO_2 forces permanent changes in the ocean heat flux convergence, which would mean that ΔT_{eq} may never quite reach the ECS of the CCSM4-NEWSOM, even if the global annual mean ocean heat uptake reaches zero.

Similarly, the unphysical forcings in the CCSM3-OLDSOM suppress ΔT_{eq} because, like the ocean heat uptake in CCSM-OGCM, the unphysical forcings remove heat from the atmosphere in regions of above average positive feedback.

Gregory et al. (2004) suggested another way of estimating the effective climate sensitivity of a climate model can be obtained by regressing $\Delta T(t)$ on $\Delta R(t)$ and extrapolating the regression to $\Delta R = 0$. The method is attractive because it requires no a priori estimate of R_f . For the 309-yr instant doubling integration of CCSM4, Gregory et al.'s method gives an effective climate sensitivity of 2.80°C (see Fig. 13), which is nearly identical to the average of the last 30 years of ΔT_{eff} from Fig. 11b (2.78°C) using the method of Murphy (1995). The excellent agreement can be seen graphically as the near intersection of dashed and dot-dashed lines at $\Delta R = 0$ in Fig. 13.

5. Conclusions

The equilibrium climate sensitivity of the CCSM4 from doubling CO_2 is 3.20°C for 1° horizontal resolution

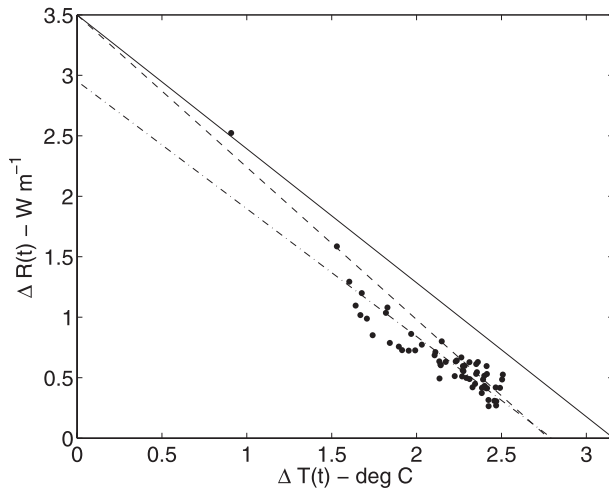


FIG. 13. Scatterplot of global mean TOA radiative balance against surface air temperature for pentadal averages of the CCSM4 instant CO_2 -doubling experiment. The solid line is through $[0, R_f]$ and $[\Delta T_{\text{eq}}, 0]$, the dashed line is through $(0, R_f)$ and $[\Delta T_{\text{eff}} (280\text{--}309), \Delta R_{\text{eff}} (280\text{--}309)]$, and the dot-dashed line is the regression line.

in each component. This is about a half degree Celsius higher than was cited for CCSM3 by Kiehl et al. (2006) and Randall et al. (2007). When comparing runs of with the same slab-ocean formulation, the ECS of the CCSM4 is higher than in CCSM3 by about 0.35°C . Climate sensitivity is higher in CCSM4 primarily owing to a reduction in warming in the upper troposphere relative to the surface warming at all latitudes. The next most important factor is an increase in shortwave cloud feedback, which is primarily the result of a relative reduction in low cloud expansion from doubling CO_2 in CCSM4 compared to CCSM3. These changes are a result of modifications to the convective cloud scheme. Adjustments to the parameterization of snow burial of vegetation increase ECS by 0.20°C , mostly due to greater warming of high northern land surfaces. The ECS in the CCSM4 would be even higher if it were not for the change in baseline CO_2 level (CCSM4's climate sensitivity is relative to a preindustrial climate while CCSM3's is present day) and the new freeze-dry cloud parameterization.

The formulation of the slab ocean in CCSM4 is substantially revised from the SOM that was released with CCSM3. We implemented the NEWSOM formulation in CCSM3 so we could isolate its effect in a model with the same physics otherwise. The new formulation causes as much as a 0.25°C increase in ECS, with regional warming that is $1^\circ\text{--}3^\circ\text{C}$ greater in the polar regions and $0.5^\circ\text{--}3^\circ\text{C}$ less in the eastern tropical Pacific and western North Atlantic. We identified unphysical forcings due to on-the-fly adjustments to the prescribed ocean heat

transport convergence and from neglecting the latent heat of snow falling into the ocean in CCSM3-OLDSOM that suppress ECS by almost 0.5°C . The fact that this is more than the difference between the CCSM3-OLDSOM and CCSM3-NEWSOM at similar resolutions is an indication that the difference in mean state of the SST and sea ice between the two formulations also influences ECS by about 0.25°C .

The NEWSOM in CCSM4 (or CCSM3) attempts to reproduce the SST and sea ice climatology from an integration of the CCSM4 (or CCSM3) with a full-depth OGCM, while the OLDSOM in CCSM3 attempts to reproduce an observed SST and sea ice climatology. The NEWSOM is integrated with the same sea ice model as in the OGCM, which by default includes sea ice dynamics, while sea ice in the OLDSOM is motionless. The new features of the NEWSOM offer an estimate of the ECS that is potentially more consistent with the surface temperature change using the CCSM4 with an OGCM run to equilibrium. Indeed the ECS in CCSM3-NEWSOM agrees within 0.01°C with the surface temperature change 3000 years after instantly doubling CO_2 in an integration of CCSM3 with an OGCM (see Danabasoglu and Gent 2009), in integrations at the same resolution.

In integrations with an OGCM where CO_2 is ramped and then stabilized at double its starting value, the transient climate response and effective climate sensitivity of CCSM3 and CCSM4 scale by the same factor relative to the ECS of the corresponding SOM version (CCSM3-NEWSOM and CCSM4-NEWSOM). The TCR is 0.54 times the ECS, and the effective climate sensitivity at the time of CO_2 doubling is 0.83 times the ECS.

We argue that these factors are controlled by the spatial pattern of ocean heat uptake, which on the zonal mean is broadly the same in CCSM3 and CCSM4. Ocean heat uptake suppresses the local surface warming with a spatial pattern that matters because feedbacks also vary spatially. Suppressing warming where feedbacks are most positive is most effective at suppressing TCR (and hence effective climate sensitivity). In the case of CCSM3 and CCSM4, the ocean heat uptake is highest just equatorward of the sea ice edge, where feedbacks are on average more positive than they are globally.

When we examined the transient response in more detail in the CCSM4, we found that the effective climate sensitivity increases over time, which we attribute to the fact that the ocean heat uptake decreases faster in the region just equatorward of the sea ice edge than it does globally.

The intermodel range of ECS among models analyzed in the IPCC AR4 (Table 8.2, Randall et al. 2007) is $2.1^\circ\text{--}4.4^\circ\text{C}$, which is nearly three times greater than the range

of ECS among CCSM3 and CCSM4 runs at the various resolutions and slab-ocean formulations listed in Table 2. The principle reason cited for the spread among models in IPCC AR4 is disagreement in the magnitude of cloud feedback. While for CCSM3 and CCSM4, differences in the combined lapse-rate and water vapor feedbacks are just as important as differences in cloud feedback. Among IPCC AR4 models, the ECS of CCSM3-OLDSOM was tied for fourth lowest with three other models out of 19 total. The ECS of CCSM4-NEWSOM would have been squarely in the middle of the pack. The TCR of CCSM3-OGCM was also tied for fourth lowest with three other models out of 19 in the IPCC AR4 (Randall et al. 2007, Table 8.2). The TCR of CCSM4-OGCM would have been slightly above the median, tied for 11th lowest.

Acknowledgments. We thank David Lawrence for advice and code changes to test the snow burial rate parameterization. We thank Kelly McCusker and Michael Winton for helpful discussions and two anonymous reviewers whose comments substantially improved this paper. The authors gratefully acknowledge the support of the National Science Foundation through Grants ARC-0909313 and ARC-0938204 (CMB), ATM-0904092 (KMS), and ARC-0908675 (PRG and DAB) and the Department of Energy through Grant FG02-07ER64433 (CMB). Computing resources were provided by the Climate Simulation Laboratory at NCAR's Computational and Information Systems Laboratory (CISL). NCAR and CISL are sponsored by the National Science Foundation and other agencies.

REFERENCES

- Bitz, C. M., 2008: Some aspects of uncertainty in predicting sea ice thinning. *Sea Ice Decline*, E. deWeaver, C. M. Bitz, and B. Tremblay, Eds., Amer. Geophys. Union, 63–76.
- , and G. H. Roe, 2004: A mechanism for the high rate of sea ice thinning in the Arctic Ocean. *J. Climate*, **17**, 3623–3631.
- , P. R. Gent, R. A. Woodgate, M. M. Holland, and R. Lindsay, 2006: The influence of sea ice on ocean heat uptake in response to increasing CO₂. *J. Climate*, **19**, 2437–2450.
- Boer, G. J., and B. Yu, 2003a: Climate sensitivity and climate state. *Climate Dyn.*, **21**, 167–176.
- , and —, 2003b: Climate sensitivity and response. *Climate Dyn.*, **20**, 415–429.
- , and —, 2003c: Dynamic climate sensitivity. *Geophys. Res. Lett.*, **30**, 1135, doi:10.1029/2002GL016549.
- Briegleb, B. P., and B. Light, 2007: A Delta–Eddington multiple scattering parameterization for solar radiation in the sea ice component of the Community Climate System Model. NCAR Tech. Note 472+STR, 100 pp.
- Collins, W. D., and Coauthors, 2006: The Community Climate System Model, version 3 (CCSM3). *J. Climate*, **19**, 2122–2143.
- Comiso, J. C., 1990: DMSP SSM/I daily and monthly polar gridded bootstrap sea ice concentrations 1990–99. National Snow and Ice Data Center, Boulder, CO, digital media. [Available online at <http://nsidc.org/data/nsidc-0002.html>.]
- Danabasoglu, G., and P. R. Gent, 2009: Equilibrium climate sensitivity: Is it accurate to use a slab ocean model? *J. Climate*, **22**, 2494–2499.
- , S. Bates, B. P. Briegleb, S. R. Jayne, M. Jochum, W. G. Large, S. Peacock, and S. G. Yeager, 2012: The CCSM4 ocean component. *J. Climate*, **25**, 1361–1389.
- Gent, P., and Coauthors, 2011: The Community Climate System Model, version 4. *J. Climate*, **24**, 4973–4991.
- Gregory, J. M., and Coauthors, 2004: A new method for diagnosing radiative forcing and climate sensitivity. *Geophys. Res. Lett.*, **31**, L03205, doi:10.1029/2003GL018747.
- Hansen, J., M. Sato, and R. Ruedy, 1997: Radiative forcing and climate response. *J. Geophys. Res.*, **102**, 6831–6864.
- Holland, M. M., and C. M. Bitz, 2003: Polar amplification of climate change in the Coupled Model Intercomparison Project. *Climate Dyn.*, **21**, 221–232.
- , —, and A. Weaver, 2001: The influence of sea ice physics on simulations of climate change. *J. Geophys. Res.*, **106**, 2441–2464.
- , —, E. C. Hunke, W. H. Lipscomb, and J. L. Schramm, 2006: Influence of the sea ice thickness distribution on polar climate in CCSM3. *J. Climate*, **19**, 2398–2414.
- , D. Bailey, B. Briegleb, B. Light, and E. Hunke, 2012: Improved sea ice shortwave radiation physics in CCSM4: The impact of melt ponds and aerosols on Arctic sea ice. *J. Climate*, **25**, 1413–1430.
- IPCC, 1990: *Climate Change: The IPCC Scientific Assessment*. Cambridge University Press, Cambridge, 365 pp.
- Kay, J., M. Holland, C. Bitz, A. Gettleman, E. Blanchard-Wrigglesworth, A. Conley, and D. Bailey, 2012: The influence of local feedbacks and northward heat transport on the equilibrium Arctic climate response to increased greenhouse gas forcing. *J. Climate*, in press.
- Kiehl, J. T., W. D. Collins, J. J. Hack, and C. Shields, 2006: The climate sensitivity of the Community Climate System Model, version 3 (CCSM3). *J. Climate*, **19**, 2584–2596.
- Knutson, T., cited 2009: FMS slab ocean model technical documentation. [Available online at <http://www.gfdl.noaa.gov/fms-slab-ocean-model-technical-documentation/>.]
- Lawrence, D. M., K. W. Oleson, M. G. Flanner, C. G. Fletcher, P. J. Lawrence, S. Levis, S. C. Swenson, and G. B. Bonan, 2012: The CCSM4 land simulation, 1850–2005: Assessment of surface climate and new capabilities. *J. Climate*, **25**, 2240–2260.
- Lunt, D. J., A. M. Haywood, G. A. Schmidt, U. Salzmann, P. J. Valdes, and H. J. Dowsett, 2010: Earth system sensitivity inferred from Pliocene modelling and data. *Nat. Geosci.*, **3**, 60–64.
- McCusker, K., D. Battisti, and C. M. Bitz, 2012: The climate response to stratospheric sulfate injections and implications for addressing climate emergencies. *J. Climate*, **25**, 3096–3116.
- McFarlane, N. A., G. J. Boer, J.-P. Blanchet, and M. Lazare, 1992: The Canadian Climate Centre second-generation general circulation model and its equilibrium climate. *J. Climate*, **5**, 1013–1044.
- Murphy, D. M., 1995: Transient response of the Hadley Centre coupled ocean–atmosphere model to increasing carbon dioxide: Part III. Analysis of global-mean response using simple models. *J. Climate*, **8**, 495–514.
- Neale, R. B., J. H. Richter, and M. Jochum, 2008: The impact of convection on ENSO: From a delayed oscillator to a series of events. *J. Climate*, **21**, 5904–5924.

- , and Coauthors, 2010: Description of the NCAR Community Atmosphere Model (CAM 4.0). NCAR Tech. Note NCAR/TN-485+STR, 212 pp. [Available online at http://www.cesm.ucar.edu/models/ccsm4.0/cam/docs/description/cam4_desc.pdf.]
- Randall, D. A., and Coauthors, 2007: Climate models and their evaluation. *Climate Change 2007: The Physical Science Basis*, S. Solomon et al., Eds., Cambridge University Press, 589–662.
- Richter, J. H., and P. J. Rasch, 2008: Effects of convective momentum transport on the atmospheric circulation in the Community Atmosphere Model, version 3. *J. Climate*, **21**, 1487–1499.
- Rind, D., R. Healy, C. Parkinson, and D. Martinson, 1997: The role of sea ice in 2XCO₂ climate model sensitivity. Part II: Hemispheric dependencies. *Geophys. Res. Lett.*, **24**, 1491–1494.
- Schmidt, G. A., and Coauthors, 2006: Present-day atmospheric simulations using GISS ModelE: Comparison to in situ, satellite, and reanalysis data. *J. Climate*, **19**, 153–192.
- Senior, C. A., and J. F. B. Mitchell, 2000: The time-dependence of climate sensitivity. *Geophys. Res. Lett.*, **27**, 2685–2688.
- Shell, K., J. T. Kiehl, and C. Shields, 2008: Using the radiative kernel technique to calculate climate feedbacks in NCAR's Community Atmosphere Model. *J. Climate*, **21**, 2269–2282.
- Soden, B., and I. Held, 2006: An assessment of climate feedbacks in coupled ocean–atmosphere models. *J. Climate*, **19**, 3354–3360.
- , —, R. Colman, K. Shell, J. Kiehl, and C. Shields, 2008: Quantifying climate feedbacks using radiative kernels. *J. Climate*, **21**, 3504–3520.
- Vavrus, S. J., and D. Waliser, 2008: An improved parameterization for simulating Arctic cloud amount in the CCSM3 climate model. *J. Climate*, **21**, 5673–5687.
- Williams, K., A. Keen, J. Crossley, C. Senior, and C. Hewitt, 2000: The slab model. Unified Model Documentation Paper 058, 27 pp. [Available online at <http://cms.ncas.ac.uk/index.php/component/content/article/56-general/1494-met-office-docs>.]
- Winton, M., K. Takahashi, and I. Held, 2010: Importance of ocean heat uptake efficacy to transient climate change. *J. Climate*, **23**, 2333–2344.
- Yi, D., and J. Zwally, 2010: Arctic sea ice freeboard and thickness. National Snow and Ice Data Center, Boulder, CO, digital media. [Available online at <http://nsidc.org/data/nsidc-0393.html>.]
- Zhang, G., and N. McFarlane, 1995: Role of convective-scale momentum transport in climate simulation. *J. Geophys. Res.*, **100**, 1417–1426.